Modeling and control of underwater vehicle: Sparus

Students:
Ahmed Borchani
Hyejoo Kwon

Course Title: Robotics Modeling

Instructor:
Mathieu Richier

Submitted on January 9, 2025

Contents

1 Introduction

This report focuses on the modeling and simulation of the Sparus, an autonomous underwater vehicle (AUV) designed for tasks such as underwater monitoring and marine research. We examine its design, propulsion, and control systems to better understand how it operates under various underwater conditions. By using mathematical models and simulations, we analyze its performance and behavior. Each section of this report addresses specific questions, and provides simple explanations of the related concepts. Through this study, we particularly highlight the movement of each part of the Sparus based on its mass and drag matrices. Additionally, we discuss the fundamental theories and equations related to the transformation of coordinates and the rigid body mass matrix.

2 Measurements

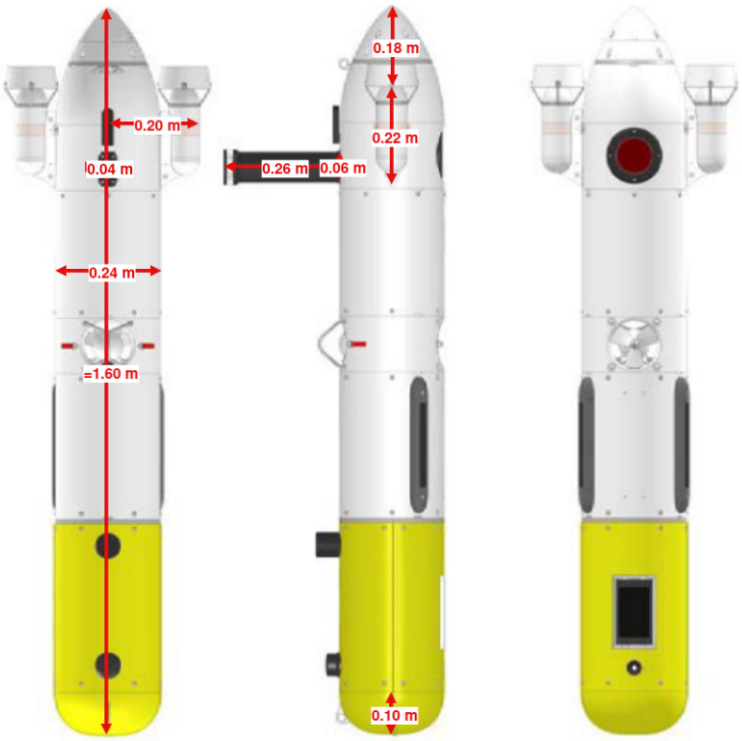

Figure 1: Sparus AUV measurements

3 Rigid body mass matrix

In this section, we will analyze the given global real mass matrix. For better understanding, the mass matrix is broken down into four parts. Each part is influenced by the effects of the AUV's mass, rotation, and inertia.

$$\mathbf{M}_{\mathbf{RB}}^{\mathbf{CO}} = \begin{bmatrix} \mathbf{M_m} & \mathbf{M_c} \\ \mathbf{M_r} & \mathbf{I} \end{bmatrix} = \left[\begin{array}{ccc|ccc} 52 & 0 & 0 & 0 & -0.1 & 0 \\ 0 & 52 & 0 & 0.1 & 0 & -1.3 \\ 0 & 0 & 52 & 0 & 1.3 & 0 \\ \hline 0 & 0.1 & 0 & 0.5 & 0 & 0 \\ -0.1 & 0 & 1.3 & 0 & 9.4 & 0 \\ 0 & -1.3 & 0 & 0 & 0 & 9.5 \end{array}\right]$$

3.1 $\mathbf{M_m}$: Mass Matrix

The mass matrix represents the relationship between forces in the x, y, and z directions and the linear accelerations in the x, y, and z directions. Each term in this matrix is derived from the object's mass distribution along these axes.

$$\mathbf{M_m} = \begin{bmatrix} 52 & 0 & 0 \\ 0 & 52 & 0 \\ 0 & 0 & 52 \end{bmatrix}$$

- 52: The mass of the rigid body. The diagonal terms show that the mass distribution in the x, y, and z directions is uniform.
- 0: There is no coupling between movements in different directions. It means that the mass is independent of cross-axis interactions.

3.2 $\mathbf{M_c}$ and $\mathbf{M_r}$: Coupling Matrices

The coupling matrices describe the interaction between linear motion and rotational motion.

$$\mathbf{M_c} = \begin{bmatrix} 0 & -0.1 & 0 \\ 0.1 & 0 & -1.3 \\ 0 & 1.3 & 0 \end{bmatrix}$$

- 0: There is no coupling between angular accelerations and forces about specific rotational axes. For example, angular acceleration q (pitch) does not generate a force about the z-axis.
- -0.1: The coupling effect of angular acceleration q (pitch) on the linear force F_x in the x-axis.
- 0.1: The coupling effect of angular acceleration p (roll) on the linear force F_y in the y-axis.
- -1.3: The influence of angular acceleration r (yaw) on the linear force F_y.
- 1.3: The influence of angular acceleration r (yaw) on the linear force F_z in the z-axis.

$$\mathbf{M_r} = \begin{bmatrix} 0 & 0.1 & 0 \\ -0.1 & 0 & 1.3 \\ 0 & -1.3 & 0 \end{bmatrix}$$

$\mathbf{M_r}$ can be described similarly to $\mathbf{M_c}$, but it represents the coupling effects in the opposite direction.While $\mathbf{M_c}$ explains how angular accelerations influence linear forces, $\mathbf{M_r}$ describes how linear accelerations generate moments or torques around rotational axes.

3.3 I: Inertia Matrix

Inertia matrix is the rigid body's rotational inertia derived from mass relative to the rotation axes.

$$\mathbf{M_I} = \begin{bmatrix} 0.5 & 0 & 0 \\ 0 & 9.4 & 0 \\ 0 & 0 & 9.5 \end{bmatrix}$$

- 0.5: The rotational inertia of the body about the x-axis. It means that there is resistance to angular acceleration around this axis.
- 9.4: The rotational inertia about the y-axis. It means that the resistance to angular acceleration is bigger than the x-axis.
- 9.5: The rotational inertia about the z-axis
- 0: Zero indicates that there is no cross-coupling between rotations around different axes.

4 Added mass matrices

In this report, we calculate the added mass matrices for the Sparus vehicle, a slender body with rotational symmetry. We use several theories to estimate the total added mass, breaking down the vehicle into its main components—hull and antenna—and calculating the added mass for each separately.

4.1 Added Mass Calculation for Hull

The Sparus hull is considered to be rotationally symmetric along the x-axis, with symmetry in both port-starboard and top-bottom directions. This symmetry allows the added mass matrix to simplify, resulting in the following matrix:

M_{hull}	1	2	3	4	5	6
1	$m11$					
2		$m_{22} = \int_L a_{22}\,dx$				$m_{26} = \int_L x\,a_{22}\,dx$
3			$m_{33} = \int_L a_{33}\,dx$		$m_{35} = -\int_L x\,a_{33}\,dx$	
4				$m_{44} = \int_L a_{44}\,dx$		
5			$m_{53} = -\int_L x\,a_{33}\,dx$		$m_{55} = \int_L x^2\,a_{33}\,dx$	
6		$m_{62} = \int_L x\,a_{22}\,dx$				$m_{66} = \int_L x^2\,a_{22}\,dx$

Since the added mass matrix for a slender body does not include an equation for M_{11}, we apply Lamb's k-factor for a spheroid. The formula for M_{11} is as follows:

$$m_{11} = k_1 \cdot \frac{4}{3} \cdot \pi \cdot \rho \cdot a \cdot b^2$$

The parameters supporting this formula are as follows :

$$\alpha_0 = \frac{2(1-e^2)}{e^3}\left(\frac{1}{2}\ln\frac{1+e}{1-e} - e\right), \quad e = \sqrt{1-\frac{b^2}{a^2}}, \quad k_1 = \frac{\alpha_0}{2-\alpha_0}$$

In order to obtain other added mass, the hull should be broken down into four parts—hemisphere,

cylinder, fin, and cone—for proper integration. The added mass is calculated based on the fundamental equation described below, using added mass coefficients for two-dimensional bodies. The areas and coefficients of the hemisphere, cylinder, and cone are considered circular in shape. However, for the fin, the area uses the same equation, but the coefficient incorporates the shape of the fin.

The equations are as follows:

$$m_a = \rho \cdot C_A \cdot A_R$$

$$A_R = \pi \cdot a^2$$

$$C_A \text{ for fin: } 1 - \left(\frac{a}{b}\right)^2 + \left(\frac{a}{b}\right)^4$$

$$C_A \text{ for hemisphere, cylinder and cone: } 1$$

The final equations of M22, M33 is :

Hemisphere	$a_1 = \int_{L/2-l_h}^{L/2} \pi\rho \left(l_h^2 - \left(x - \frac{L}{2} + l_h\right)^2\right) dx$
Cylinder	$a_2 = \int_{-(L/2-l_t-l_{co})}^{L/2-l_h} \pi\rho R^2 dx$
Fins	$a_3 = \int_{-(L/2-l_{co})}^{-(L/2-l_t-l_{co})} \pi\rho R_f^2 \left(1 - \left(\frac{R}{R_f}\right)^2 + \left(\frac{R}{R_f}\right)^4\right) dx$
Cone	$a_4 = \int_{-L/2}^{-(L/2-l_{co})} \pi\rho \left(\frac{R}{l_{co}}\left(x + \frac{L}{2} - l_{co}\right) + R\right)^2 dx$
Added Mass (m_{22}, m_{33})	$m_{22} = m_{33} = a_1 + a_2 + a_3 + a_4$

Other terms such as M26, M35, M55, M66 etc can be derived by multiplying x or x^2 into the m_{22} equation. By summing all these elements, the added mass for the hull was computed, resulting in the following outcome :

$$m_{\text{hull}} = \begin{bmatrix} 1.8621 & 0 & 0 & 0 & 0 & 0 \\ 0 & 75.8479 & 0 & 0 & 0 & -3.6469 \\ 0 & 0 & 75.8479 & 0 & 3.6469 & 0 \\ 0 & 0 & 0 & 0 & 0 & 0 \\ 0 & 0 & 3.6469 & 0 & 14.1013 & 0 \\ 0 & -3.6469 & 0 & 0 & 0 & 14.1013 \end{bmatrix}$$

4.2 Added Mass of the Antenna

The antenna is identified as having a spheroid shape. However, the z-axis is the longitudinal axis of this body. Therefore, we recalculated the added mass matrix along the z-axis and applied the same method to derive the added mass coefficients by summing the area of the antenna. The matrix is as follow :

M_A	1	2	3	4	5	6
1	$m_{11} = \int_L a_{11} dz$				$m_{15} = \int_L z\, a_{11}\, dz$	
2		$m_{22} = \int_L a_{22}\, dz$		$m_{24} = -\int_L z a_{22} dz$		
3						
4		$m_{42} = -\int_L z a_{22} dz$		$m_{44} = \int_L z^2\, a_{22}\, dz$		
5	$m_{51} = \int_L z a_{11} dz$				$m_{55} = \int_L z^2\, a_{11}\, dz$	
6						$m_{66} = \int_L a_{66}$

Since the top left 3×3 matrices of the added mass for the antenna have significant values, other terms can be considered negligible. As a result, we take into account only two terms, which are as follows:

$$m_{11} = \int_{-h/2}^{h/2} \pi \rho C_A l_1^2\, dz$$

$$m_{22} = \int_{-h/2}^{h/2} \pi \rho C_A l_2^2\, dz$$

The final added mass matrix for the antenna is the following:

$$M_{\text{Antenna}} = \begin{bmatrix} 0.7286 & 0 & 0 & 0 & 0 & 0 \\ 0 & 1.4556 & 0 & 0 & 0 & 0 \\ 0 & 0 & 0 & 0 & 0 & 0 \\ 0 & 0 & 0 & 0 & 0 & 0 \\ 0 & 0 & 0 & 0 & 0 & 0 \\ 0 & 0 & 0 & 0 & 0 & 0 \end{bmatrix}$$

By combining the derived added mass of the hull and antenna, the final added mass is obtained as follows:

$$M_A^{CB} = \begin{bmatrix} 2.5907 & 0 & 0 & 0 & 0 & 0 \\ 0 & 77.3035 & 0 & 0 & 0 & -3.6469 \\ 0 & 0 & 75.8479 & 0 & 3.6469 & 0 \\ 0 & 0 & 0 & 0 & 0 & 0 \\ 0 & 0 & 3.6469 & 0 & 14.1013 & 0 \\ 0 & -3.6469 & 0 & 0 & 0 & 14.1013 \end{bmatrix}$$

5 Transformation from gravity center to buoyancy center

As a first step to get the global mass matrix at the gravity center (CG), we need to transform the added mass matrices to be computed at the same center.

The added masses matrices are computed at the center of buoyancy (CB) of the bodies. For the thrusters and the antenna, the CG and CB are considered to coincide. However, for the main body they are different, based on the provided coordinates the distance between CG and CB is described in meters by the vector:

$$\mathbf{r}_{CG}^{CB} = \begin{bmatrix} 0 \\ 0 \\ -0.02 \end{bmatrix}$$

To get theses matrices relative to the center of gravity, the following equation is used:

$$M_A^{CB} = H^T\left(\mathbf{r}_{CG}^{CB}\right) M_A^{CG} H\left(\mathbf{r}_{CG}^{CB}\right) \tag{1}$$

where H is the following transformation matrix:

$$H(\mathbf{r}) = \begin{bmatrix} I_{3\times3} & S^T(\mathbf{r}) \\ 0_{3\times3} & I_{3\times3} \end{bmatrix}$$

($S^T(\mathbf{r})$ is the transpose of a skew matrix for the distance vector $\mathbf{r}$)

The distance that separates the CB (or CG) of the thrusters and antenna from the CG of the main body is needed to transform their added masses matrices.

- Distance between CG of right thruster and CG of main body in meters is:

$$\mathbf{r}_{right\_thruster} = \begin{bmatrix} -0.59 \\ 0.17 \\ 0 \end{bmatrix}$$

- Distance between CG of left thruster and CG of main body in meters is:

$$\mathbf{r}_{left\_thruster} = \begin{bmatrix} -0.59 \\ -0.17 \\ 0 \end{bmatrix}$$

- Distance between CG of Antenna and CG of main body in meters is:

$$\mathbf{r}_{antenna} = \begin{bmatrix} -0.4 \\ 0 \\ -0.15 \end{bmatrix}$$

6 Comparison

6.1 CG vs CB

The matrices $\mathbf{M_{RB}^{CG}}$ and $\mathbf{M_{RB}^{CB}}$ represent the mass and inertia relative to the center of gravity (CG) and buoyancy (CB). While $\mathbf{M_{RB}^{CG}}$ provides a basic framework, $\mathbf{M_{RB}^{CB}}$ includes additional

effects from the buoyancy center.

$$\mathbf{M_{RB}^{CG}} = \begin{bmatrix} 54.591 & 0 & 0 & 0 & -0.100 & 0 \\ 0 & 129.304 & 0 & 0.100 & 0 & -4.947 \\ 0 & 0 & 127.848 & 0 & 4.947 & 0 \\ 0 & 0.100 & 0 & 0.500 & 0 & 0 \\ -0.100 & 0 & 4.947 & 0 & 23.501 & 0 \\ 0 & -4.947 & 0 & 0 & 0 & 23.601 \end{bmatrix}$$

$$\mathbf{M_{RB}^{CB}} = \begin{bmatrix} 54.591 & 0 & 0 & 0 & -0.247 & 0 \\ 0 & 129.304 & 0 & 1.835 & 0 & -5.529 \\ 0 & 0 & 127.848 & 0 & 4.947 & 0 \\ 0 & 1.835 & 0 & 0.563 & 0 & -0.160 \\ -0.247 & 0 & 4.947 & 0 & 23.518 & 0 \\ 0 & -5.529 & 0 & -0.160 & 0 & 23.834 \end{bmatrix}$$

The diagonal elements of $\mathbf{M_{RB}^{CB}}$ and $\mathbf{M_{RB}^{CG}}$ are similar, showing that the mass and rotational inertia is consistent. However, off-diagonal elements such as M_{24}, M_{46}, and M_{62} in $\mathbf{M_{RB}^{CB}}$ are significant differences. For instance, M_{24} in $\mathbf{M_{RB}^{CB}}$ is 1.8353, much higher than 0.1000 in $\mathbf{M_{RB}^{CG}}$. It means that there is an additional inertia effects. Furthermore, M_{64} and M_{26} in $\mathbf{M_{RB}^{CB}}$ also have noticable changes. We found that this changes stands for the impact of the buoyancy center on the dynamic response. These variations underline the importance of $\mathbf{M_{RB}^{CB}}$ in modeling realistic vessel's behavior.

6.2 The values of the main solid with the others

$\mathbf{M_{Ahull}^{CB}}$ and $\mathbf{M_{Aantenna}^{CB}}$ are added mass matrices for the hull and the antenna, calculated based on the center of buoyancy (CB). These matrices show how the hull and antenna behave in water. They have clear differences in their values.

$$\mathbf{M_{Ahull}^{CB}} = \begin{bmatrix} 1.862 & 0 & 0 & 0 & 0 & 0 \\ 0 & 75.848 & 0 & 0 & 0 & -3.647 \\ 0 & 0 & 75.848 & 0 & 3.647 & 0 \\ 0 & 0 & 0 & 0 & 0 & 0 \\ 0 & 0 & 3.647 & 0 & 14.101 & 0 \\ 0 & -3.647 & 0 & 0 & 0 & 14.101 \end{bmatrix}$$

$$\mathbf{M}^{\mathbf{CG}}_{\mathbf{Aantenna}} = \begin{bmatrix} 0.729 & 0 & 0 & 0 & 0 & 0 \\ 0 & 1.456 & 0 & 0 & 0 & 0 \\ 0 & 0 & 0 & 0 & 0 & 0 \\ 0 & 0 & 0 & 0 & 0 & 0 \\ 0 & 0 & 0 & 0 & 0 & 0 \\ 0 & 0 & 0 & 0 & 0 & 0 \end{bmatrix}$$

Looking at the diagonal elements, $\mathbf{M}^{\mathbf{CB}}_{\mathbf{Ahull}}$ has larger numbers, such as: $M_{22}= M_{33} = 75.848$, $M_{55} = M_{66} = 14.101$. This means the hull resists movement and rotation in water more strongly.

In contrast, $\mathbf{M}^{\mathbf{CB}}_{\mathbf{Aantenna}}$ has smaller numbers, such as: $M_{11} = 0.729$, $M_{22} = 1.456$, and the other diagonal elements are 0. This shows that the antenna is less affected by water movement. For off-diagonal elements, the hull has been affected by the connection between the movement of the z-axis and the rotation of the y-axis, such as $M_{35} = 3.647$,M_{26} = -3.647. However, in $\mathbf{M}^{\mathbf{CB}}_{\mathbf{Aantenna}}$, most off-diagonal elements are 0, meaning there is almost no connection between movement and rotation.

6.3 The added vs The real mass matrix

The matrix $\mathbf{M}^{\mathbf{RB}}_{\mathbf{CO}}$ is the rigid-body mass matrix based on the center of origin (CO). $\mathbf{M}^{\mathbf{A}}_{\mathbf{CG}}$ is the added mass matrix with respect to the center of gravity (CG). These two matrices has similar structures, but has differences in both their diagonal and off-diagonal elements.

$$\mathbf{M}^{\mathbf{CO}}_{\mathbf{RB}} = \begin{bmatrix} 52 & 0 & 0 & 0 & -0.1 & 0 \\ 0 & 52 & 0 & 0.1 & 0 & -1.3 \\ 0 & 0 & 52 & 0 & 1.3 & 0 \\ 0 & 0.1 & 0 & 0.5 & 0 & 0 \\ -0.1 & 0 & 1.3 & 0 & 9.4 & 0 \\ 0 & -1.3 & 0 & 0 & 0 & 9.5 \end{bmatrix}$$

$$\mathbf{M}^{\mathbf{CG}}_{\mathbf{A}} = \begin{bmatrix} 2.591 & 0 & 0 & 0 & -0.147 & 0 \\ 0 & 77.304 & 0 & 1.735 & 0 & -4.229 \\ 0 & 0 & 75.848 & 0 & 3.647 & 0 \\ 0 & 1.735 & 0 & 0.063 & 0 & -0.160 \\ -0.147 & 0 & 3.647 & 0 & 14.118 & 0 \\ 0 & -4.229 & 0 & -0.160 & 0 & 14.334 \end{bmatrix}$$

The diagonal elements of $\mathbf{M}^{\mathbf{RB}}_{\mathbf{CO}}$ are simple and symmetric. This means the mass and rotational inertia of the rigid body are balanced. On the other hand, the diagonal elements of $\mathbf{M}^{\mathbf{A}}_{\mathbf{CG}}$ are varied. Some values are much larger, which shows the effects from fluid. This makes $\mathbf{M}^{\mathbf{A}}_{\mathbf{CG}}$ more complex.

For the off-diagonal elements, $\mathbf{M_{CO}^{RB}}$ has small values. This shows that the interaction between acceleration and forces are small. In contrast, $\mathbf{M_{CG}^{A}}$ has larger off-diagonal values. This means that fluid around vessel creates stronger interactions between acceleration and forces.

7 Drag matrices

For both the main body and the parts, the drag matrix has only values for the diagonal terms:

$$\begin{bmatrix} K_{11} & 0 & 0 & 0 & 0 & 0 \\ 0 & K_{22} & 0 & 0 & 0 & 0 \\ 0 & 0 & K_{33} & 0 & 0 & 0 \\ 0 & 0 & 0 & K_{44} & 0 & 0 \\ 0 & 0 & 0 & 0 & K_{55} & 0 \\ 0 & 0 & 0 & 0 & 0 & K_{66} \end{bmatrix}_{CB}^{Rb}$$

The coefficients are calculated based on:

- $K_{11} = \frac{1}{2}\rho S_x C_{D11}$,
- $K_{22} = \frac{1}{2}\rho C_{D22} D_y L$
- $K_{33} = \frac{1}{2}\rho C_{D33} D_z L = K_{22}$ (Due to symmetry)
- $K_{44} = 0$
- $K_{55} = \frac{1}{64}\rho L^4 C_{D33} D_z$
- $K_{66} = \frac{1}{64}\rho L^4 C_{D22} D_y = K_{55}$ (Due to symmetry)

S_x and C_{D11} are the projected surface and the 3D drag coefficient in the $\vec{x}$ direction.

D_y and C_{D22} are the characteristic width and 2D drag coefficient along the length in the $\vec{y}$ direction.

D_z and C_{D33} are the characteristic width and 2D drag coefficient along the length in the $\vec{z}$ direction.

7.1 Drag matrix of the hull

The projected surface of the hull in the $\vec{x}$ direction can be estimated to be a cylinder, thus it is:

$$S_x = \pi \cdot R^2 = 0.045m^2$$

The hull can be estimated as an ellipsoid. The fraction $L/D = 1.6/0.24 = 6.67 \approx 8$, and the flow is turbulent so the 3D coefficient is $C_{D11} = 0.1$, thus

$$K_{11} = \frac{1}{2}\rho S_x C_{D11} = 2.26$$

The 2D projection of the hull in the $\vec{y}$ direction can be estimated as a cylindrical rod $Dy = 0.24$. The 2D drag coefficient $C_{D22} = 0.3$, so:

$$K_{33} = K_{22} = \frac{1}{2}\rho C_{D22} D_y L = 57.6$$

$$K_{55} = K_{66} = 7.372$$

The final drag matrix is:

$$K^{CB}_{Hull} = \begin{bmatrix} 2.26 & 0 & 0 & 0 & 0 & 0 \\ 0 & 57.6 & 0 & 0 & 0 & 0 \\ 0 & 0 & 57.6 & 0 & 0 & 0 \\ 0 & 0 & 0 & 0 & 0 & 0 \\ 0 & 0 & 0 & 0 & 7.372 & 0 \\ 0 & 0 & 0 & 0 & 0 & 7.372 \end{bmatrix}^{Hull}_{CB}$$

7.2 Drag matrix of the antenna

The antenna is approximated to be a rectangular prism geometrically. The projected surface in the $\vec{x}$ direction is a rectangle with dimensions $L = 0.26$ and $Dx = 0.04$ so:

$$S_x = L \cdot D = 0.26 \cdot 0.04 = 0.01m^2$$

In this case, the coefficient can be calculated in the following way:

$$C_{D11} = 1.1 + 0.02 \cdot (L/D + D/L) = 1.233$$

The 2D projection of the antenna in the $\vec{y}$ direction is a rectangle with dimensions $L = 0.26$ and $Dy = 0.06$. To get the drag coefficient the fraction $0.26/0.06 = 4.3$, according to the table for rectangular rod drag coefficients:

$$C_{D22} = 1.3$$

Since the antenna is connected to the hull the drag forces along the z-axis are neglected. Additionally, for the antenna only the 3 diagonal coefficients of the top left 3*3 matrices are computed. Finally we get:

$$K_{11} = \frac{1}{2}\rho S_x C_{D11} = 6.412$$

$$K_{22} = \frac{1}{2}\rho C_{D22} D_y L = 10.14$$

$$K_{33} = K_{44} = K_{55} = K_{66} = 0$$

Therefore, the drag matrix for the antenna is:

$$K^{CB}_{antenna} = \begin{bmatrix} 6.412 & 0 & 0 & 0 & 0 & 0 \\ 0 & 10.14 & 0 & 0 & 0 & 0 \\ 0 & 0 & 0 & 0 & 0 & 0 \\ 0 & 0 & 0 & 0 & 0 & 0 \\ 0 & 0 & 0 & 0 & 0 & 0 \\ 0 & 0 & 0 & 0 & 0 & 0 \end{bmatrix}^{Antenna}_{CB}$$

The drag matrix for the thrusters is neglected since its values are too small and they don't have much of an effect.

7.3 Drag matrix of the thrusters

In the surge direction, thrusters' shape during motion can be modeled as an ellipsoid with a coefficient $C_{D11} = 0.1$. The projected surface is $S_x = \pi \cdot 0.035^2 = 0.0038$. Thus the drag coefficient is:

$$K_{11} = \frac{1}{2}\rho S_x C_{D11} = 0.19$$

In the sway direction, the drag coefficient for the thrusters is assumed to be negligible since the drag forces in that direction are mostly influenced by the hull.

In the heave direction, the 2D projected surface can be estimated to be a rectangle with dimensions 0.08 and 0.22, thus the drag coefficient along z is $C_{D33} = 1.3$

$$K_{33} = \frac{1}{2}\rho C_{D33} D_y L = 11.44$$

In addition, K_{44}, K_{55}, and K_{66} are considered negligible. They are only accounted for the hull, as their effects on the smaller peripheral parts are minimal. Therefore, the drag matrix for each of the thrusters is:

$$K^{CB}_{thruster} = \begin{bmatrix} 0.19 & 0 & 0 & 0 & 0 & 0 \\ 0 & 0 & 0 & 0 & 0 & 0 \\ 0 & 0 & 11.44 & 0 & 0 & 0 \\ 0 & 0 & 0 & 0 & 0 & 0 \\ 0 & 0 & 0 & 0 & 0 & 0 \\ 0 & 0 & 0 & 0 & 0 & 0 \end{bmatrix}^{Antenna}_{CB}$$

8 Coriolis Forces

The equation for the Coriolis force is derived from the system's inertia matrix (M) and the Coriolis-centripetal matrix. The M matrix can be defined as the global real mass matrix described in the section above, such that:

$$M = \begin{bmatrix} M_{11} & M_{12} \\ M_{21} & M_{22} \end{bmatrix} = \begin{bmatrix} 54.591 & 0 & 0 & 0 & -0.247 & 0 \\ 0 & 129.304 & 0 & 1.835 & 0 & 12.219 \\ 0 & 0 & 127.848 & 0 & -12.801 & 0 \\ 0 & 1.835 & 0 & 0.563 & 0 & 0.195 \\ -0.247 & 0 & -12.801 & 0 & 5.770 & 0 \\ 0 & 12.219 & 0 & 0.195 & 0 & 6.086 \end{bmatrix}$$

Since the Coriolis force is not affected by the linear velocity vector, v1 can be considered negligible. Therefore, the modified version of the Coriolis-centripetal matrix can be parameterized as follows:

$$C(v) = -C^T(v) = \begin{bmatrix} \mathbf{0}_{3\times3} & -S(M_{12}v_2) \\ -S(M_{12}v_2) & -S(M_{22}v_2) \end{bmatrix}$$

Based on the previous matrix, the Coriolis forces are calculated, resulting in the following:

$$\mathbf{F}_c = \mathbf{C}_{\mathrm{v}} \cdot \mathbf{V}_{\mathrm{itB}}$$

where $\mathbf{V}_{\mathrm{itB}} = [u, v, w, p, q, r]^T$ represents the body-fixed velocity.

9 Thrusters Forces

The thrusters' forces are modeled by $\mathbf{U}^b$, such that:

$$\mathbf{U}^b = \mathbf{E}^b \mathbf{F}_T^b = \mathbf{E}_{6\times3}^b \begin{bmatrix} F_{T1}^b \\ F_{T2}^b \\ F_{T3}^b \end{bmatrix}$$

where F_{T1}^b, F_{T2}^b, and F_{T3}^b represent the forces of Motor 1 (situated in the middle of the AUV), Motor 2 (the right thruster), and Motor 3 (the left thruster) respectively.

$\mathbf{E}^b$ represents the mapping matrix, which has dimensions of 6×3. The result is a vector of

forces and moments produced by the thrusters:

$$\mathbf{U}^b = \begin{bmatrix} F_x \\ F_y \\ F_z \\ M_x \\ M_y \\ M_z \end{bmatrix}$$

To find the $\mathbf{E}^b$ matrix and the $\mathbf{U}^b$ vector, the following points were visited:

- F^b_{T1} is a force in the $\vec{z}$ direction. It does not produce any moment since it is located at the coordinate (0, 0, 0.08). This can be verified by:

$$\overrightarrow{r}^b_{T1} \times \overrightarrow{F}^b_{T1} = \begin{bmatrix} 0 \\ 0 \\ 0.08 \end{bmatrix} \times \begin{bmatrix} 0 \\ 0 \\ F^b_{T1} \end{bmatrix} = \begin{bmatrix} 0 \\ 0 \\ 0 \end{bmatrix}$$

- F^b_{T2} and F^b_{T3} are forces in the $\vec{x}$ direction, that can also produce moments around the z-axis. Their distance vectors are used to calculate the moments in the following way:

$$\overrightarrow{r}^b_{T2} \times \overrightarrow{F}^b_{T2} = \begin{bmatrix} -0.59 \\ 0.17 \\ 0 \end{bmatrix} \times \begin{bmatrix} F^b_{T2} \\ 0 \\ 0 \end{bmatrix} = \begin{bmatrix} 0 \\ 0 \\ -0.17 \cdot F^b_{T2} \end{bmatrix}$$

$$\overrightarrow{r}^b_{T3} \times \overrightarrow{F}^b_{T3} = \begin{bmatrix} -0.59 \\ -0.17 \\ 0 \end{bmatrix} \times \begin{bmatrix} F^b_{T3} \\ 0 \\ 0 \end{bmatrix} = \begin{bmatrix} 0 \\ 0 \\ 0.17 \cdot F^b_{T3} \end{bmatrix}$$

Therefore the thrusters mapped vector is:

$$\mathbf{U}^b = \mathbf{E}^b \mathbf{F}^b_T = \begin{bmatrix} 0 & 1 & 1 \\ 0 & 0 & 0 \\ 1 & 0 & 0 \\ 0 & 0 & 0 \\ 0 & 0 & 0 \\ 0 & \text{-0.17} & 0.17 \end{bmatrix} \cdot \begin{bmatrix} F^b_{T1} \\ F^b_{T2} \\ F^b_{T3} \end{bmatrix} = \begin{bmatrix} F^b_{T2} + F^b_{T3} \\ 0 \\ F^b_{T1} \\ 0 \\ 0 \\ -0.17 \cdot F^b_{T2} + 0.17 \cdot F^b_{T3} \end{bmatrix}$$

10 Simulations and Measurements

10.1 Experiments for validation

To validate the derived model, it is necessary to run simulations of different scenarios, and check the motion to verify if it behaves as expected. The simulations are run for 50 seconds each.

10.1.1 Heave motion

To simulate an upward movement, the thruster in the middle of the hull is activated solely, with a power of 20%. As expected, the most significant movement is in the heave direction. In addition, a negative pitch is noticed. This is due to the influence of the damping forces (added mass and drag forces), mostly by those related to the side thrusters. The pitch influences the movement of the AUV, and is the reason behind the negative surge movement.

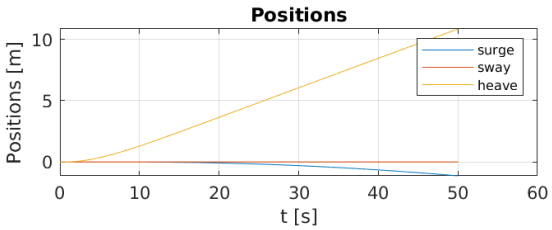

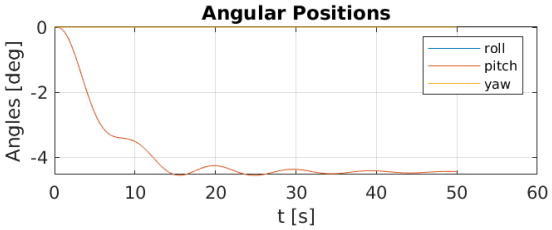

From the linear acceleration graph, it can be observed that the acceleration in the heave direction starts high but decreases significantly over time as the AUV reaches a steady velocity. The angular velocity and acceleration for the pitch shows an oscillatory behavior at the beginning, dampening over time due to the stabilizing nature of the damping forces and the PID controller.

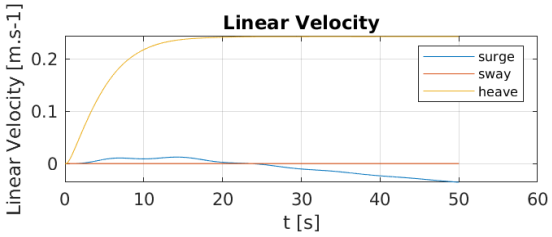

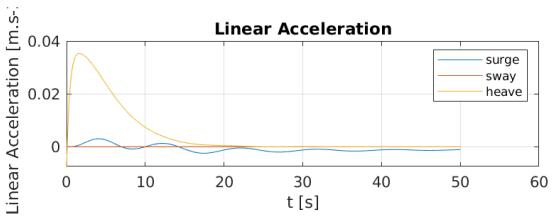

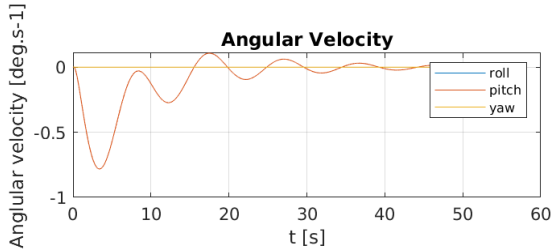

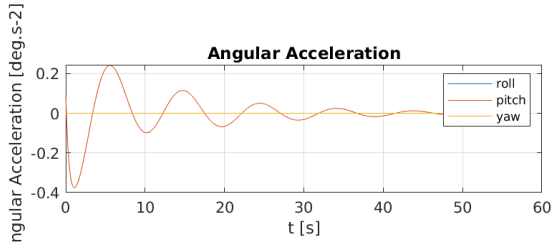

The 3D simulation of the trajectory shows how the AUV dives 8 meters in the heave direction, with a curve that results in 1 meter movement in the surge direction. The effects on the sway direction are minimal as seen in the graph:

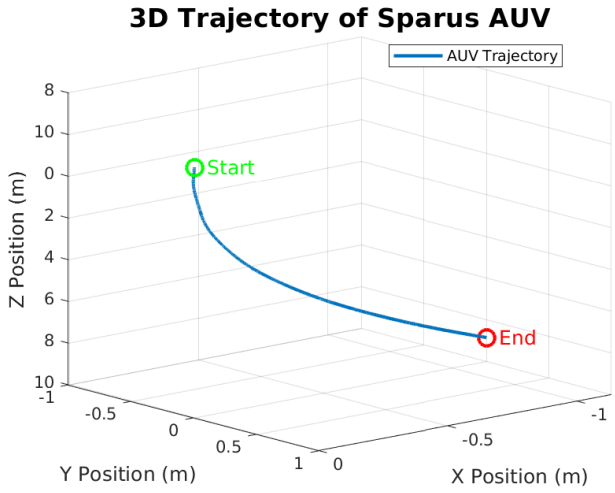

10.1.2 Surge motion

In this scenario, only the side thrusters are turned on. They are powered up to 30% of their maximum value. The AUV is moving in the surge direction with a small heave deviation. The latter is due to the damping forces, especially the ones caused by the antenna. It acts in a way that the vehicle has a positive pitch, and the thrusters keep on pushing forward so the pitch angle increases until it stabilizes.

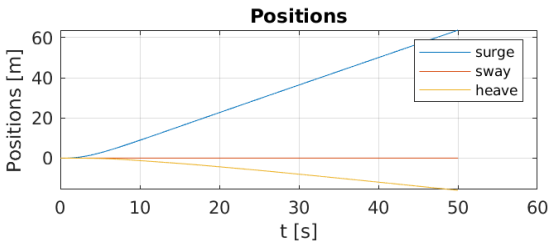

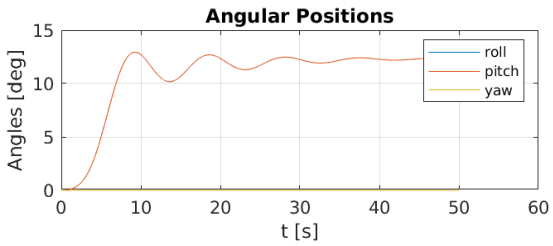

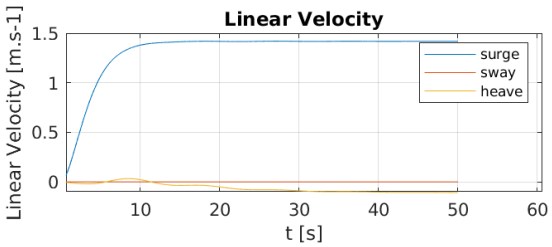

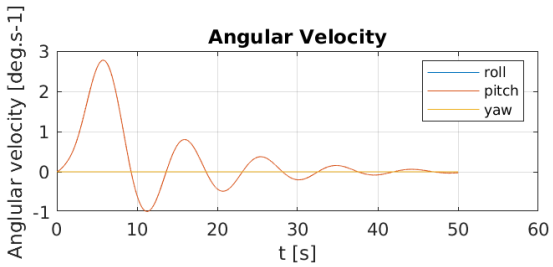

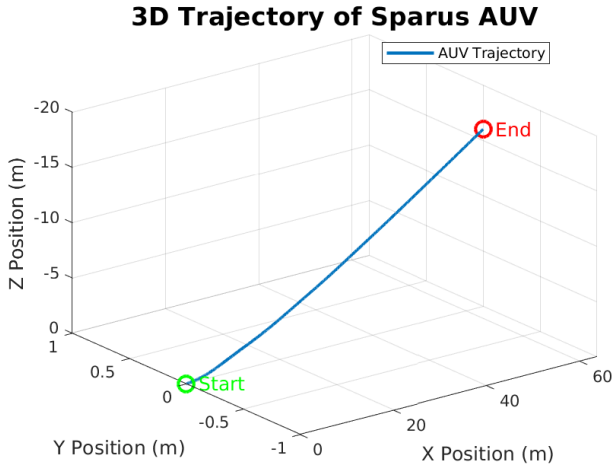

We can see that due to its buoyancy, the AUV moves up gradually. Actually if all the thrusters are turned off, the AUV will also move up due to this effect. The values in the z axis are inverted, since positive z values means a movement downwards.

10.1.3 Motion to the right

To move the AUV to the right, the left thruster is set to 30%, while the right one is set to 20%. The middle thruster is turned off. As expected, the primary motion occurs in the sway direction. However, due to the asymmetrical thrust distribution, a noticeable yaw motion is introduced, causing the AUV to curve while moving to the right.

Additionally, the drag and added mass effects contribute to angular dynamics, primarily influencing the roll motion slightly. This can be observed as a result of the thrust asymmetry. The trajectory in the 3D plot confirms a curved motion with the AUV gradually transitioning to the right in the horizontal plane.

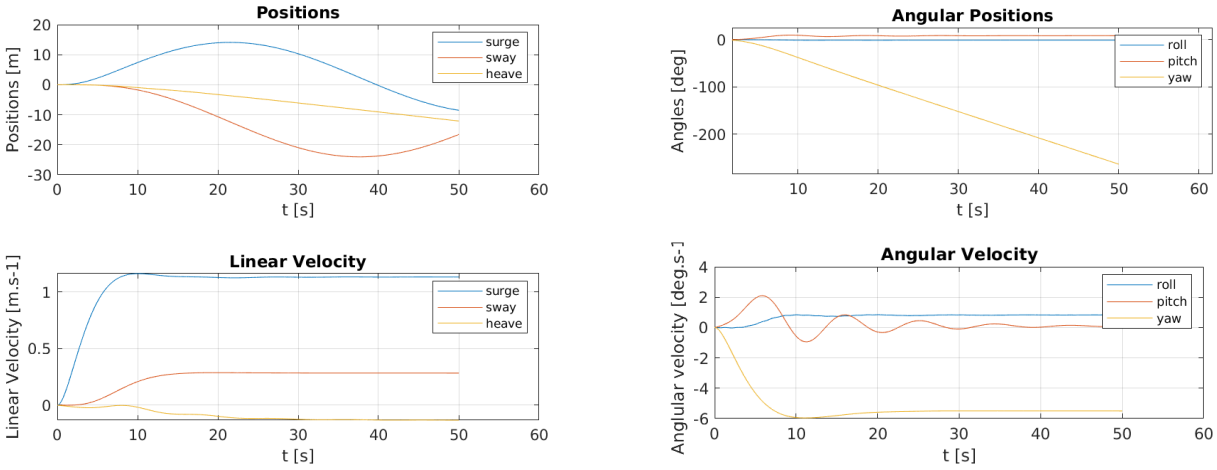

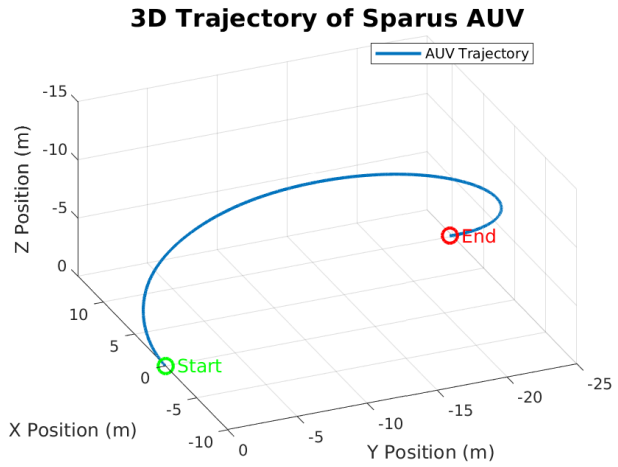

10.1.4 Motion to the left

To simulate a motion to the left, the opposite is done. The right thruster is set to 30%, while the left one is set to 20%. The same as for the right movement can be concluded due to the symmetry. The 3D motion is the following:

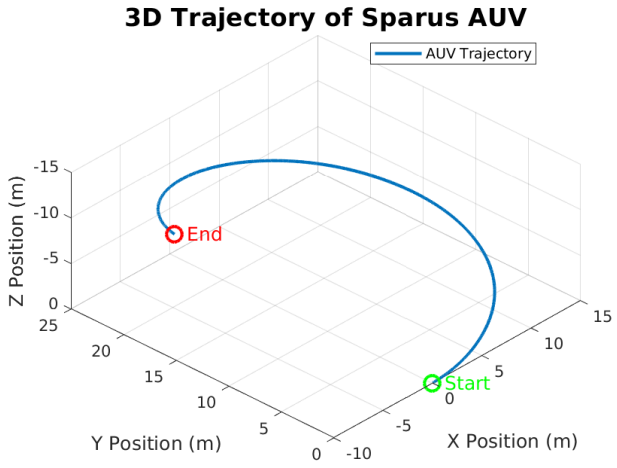

10.1.5 Using all the thrusters

To simulate forward motion, all the thrusters are activated with a power of 30%. As expected, the primary motion is in the surge direction, as evident from the linear increase in surge position over time. The sway and heave components remain small, demonstrating that the motion is effectively linear and stable.

In terms of angular dynamics, the roll, pitch, and yaw angles stabilize quickly after an initial transient response, which is caused by the initial forces and moments from the thrusters. The 3D trajectory confirms a straight-line motion, validating the stable and forward movement of the AUV.

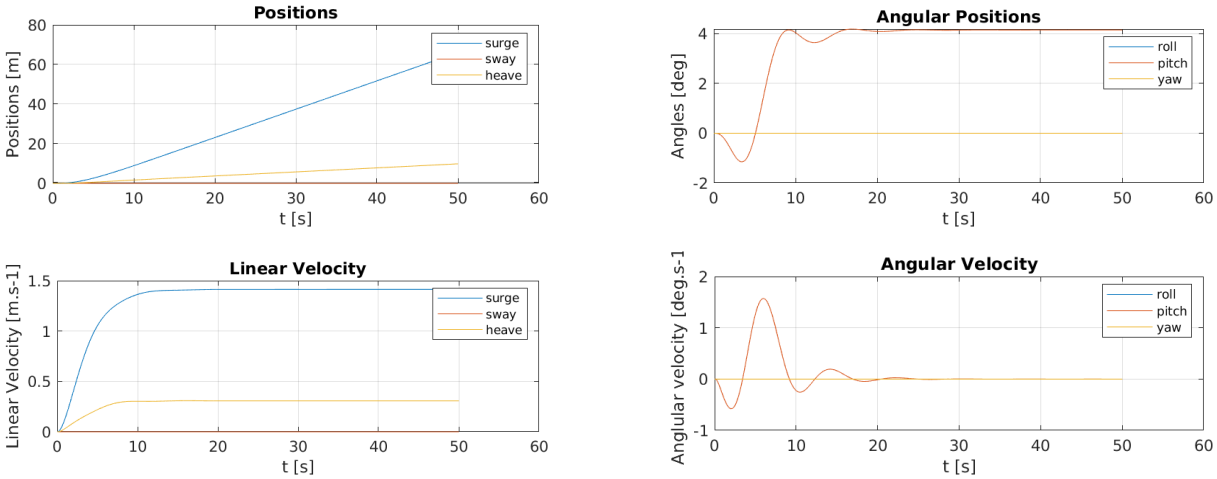

The 3D graph shows motion that seems stable and almost linear. The AUV is moving forward an important distance of 65 meters propelled by its 2 side thrusters, and it is also descending for about 10 meters. There is only 1 thruster pushing in the heave direction. In addition, the AUV's buoyancy is pushing opposite to this motion, thus the heave has a smaller value than surge.

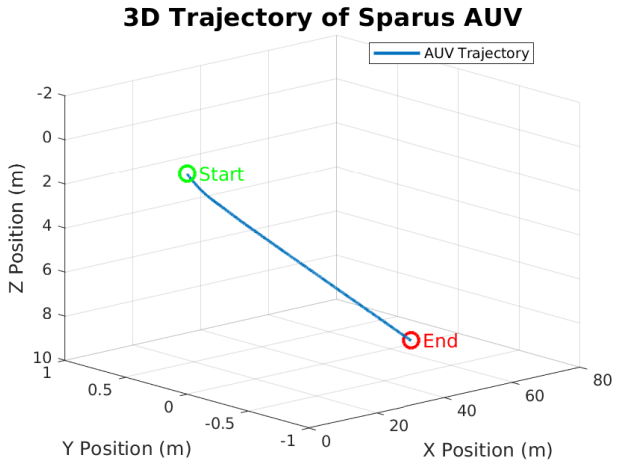

10.2 Global Mass Matrix impact

In this section, we conducted several experiments to examine the effects of the coefficients of the added mass matrix. To do this, each coefficient was removed under the same condition described above, including upward movement. When removing individual coefficients of the added mass matrix for the hull, we observed significant changes in M33 and M55. In the following chapters, we discuss the consequences of removing these values.

10.2.1 Impact of M33 on Upward Movement

When we remove the added mass coefficient for heave motion (M33), we observe that backward drift increases. This indicates an imbalance in the force distribution. We notice that the pitch angle oscillates more and takes longer to stabilize. In the angular acceleration graph, the angular acceleration increases to more than 0.8, which is four times greater than the original heave motion described above. By removing M33, we reduce damping, making the AUV more vulnerable to turbulence. This shows that m33 is critical to maintain stability, reducing oscillations.

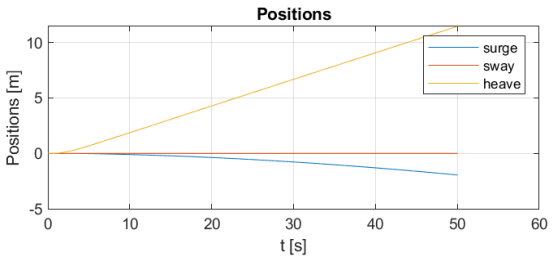

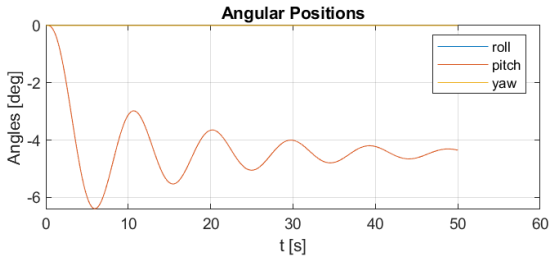

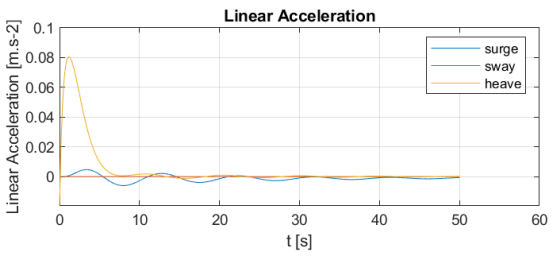

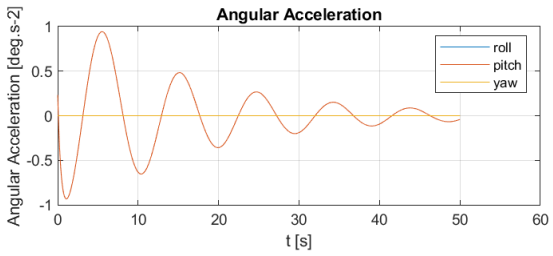

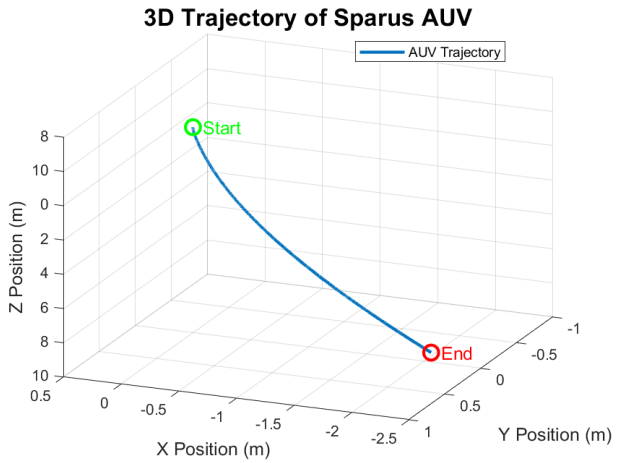

10.2.2 Impact of M55 on Upward Movement

When we removed m55, the AUV's downward motion slowed down. The final height was lower, as shown in the position graph. From the angular position and acceleration graphs, we observed larger pitch angle oscillations. Additionally, the linear acceleration of surge oscillated unevenly. This indicates that the AUV's vertical efficiency decreased because m55 plays a critical role in stabilizing the vehicle's dynamics. Without m55, the AUV's center of mass and buoyancy distribution becomes less balanced, leading to increased pitch oscillations.

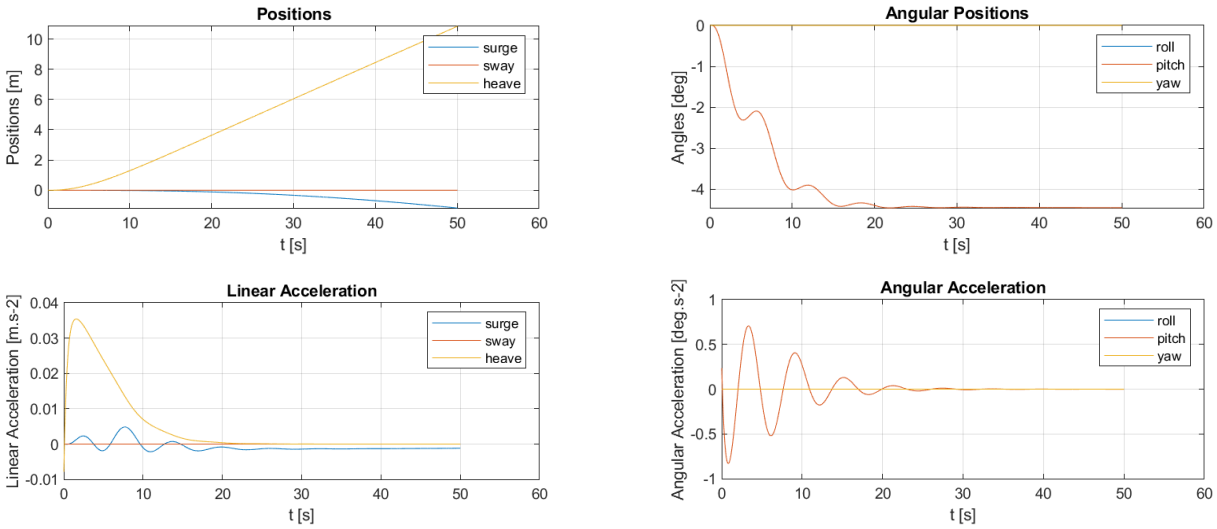

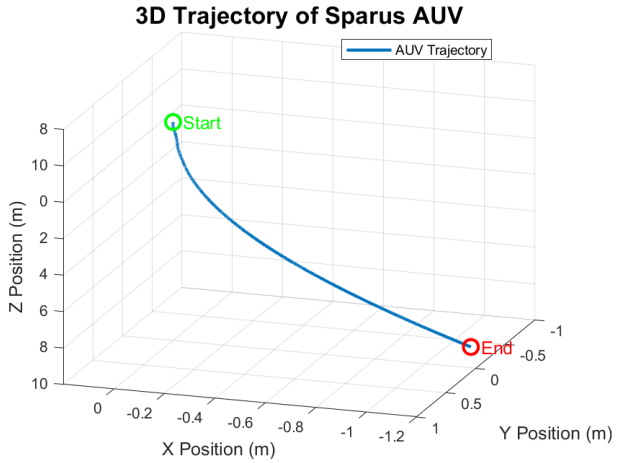

10.2.3 Impact of Added mass on Upward Movement

When we removed the added mass matrix, the AUV's motion became very unstable. In the position graph, the downward height dropped a lot, and the AUV did not descend as low as before. In the angular position graph, the pitch dropped very quickly and steeply. It stabilized faster, but the sharp drop shows the AUV could not resist the change in angle. The angular acceleration graph shows the pitch acceleration dropped sharply to -0.6 deg/s, showing very unstable movement before it settled. Overall, removing the added mass made the AUV less stable and less efficient. It lost height and showed big, quick changes in motion and angles. We saw that the added mass is very important for keeping the AUV balanced and stable.

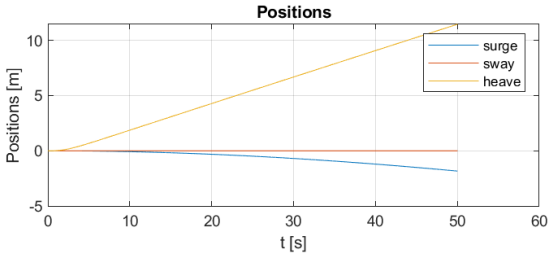

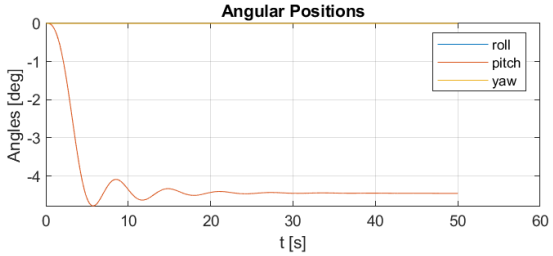

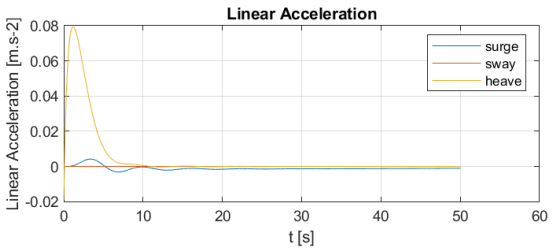

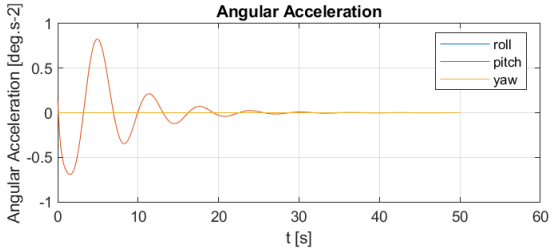

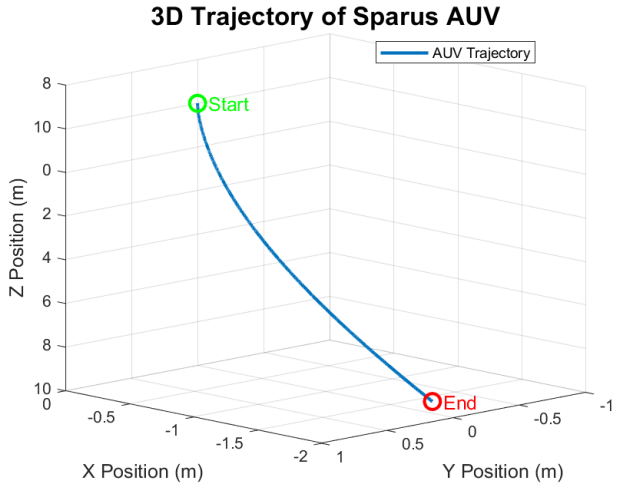

10.3 Drag forces impact

10.3.1 Impact of the hull's drag forces

If the hull's drag force is completely removed and the scenario with only the middle thruster activated is repeated, the resulting graphs are shown below:

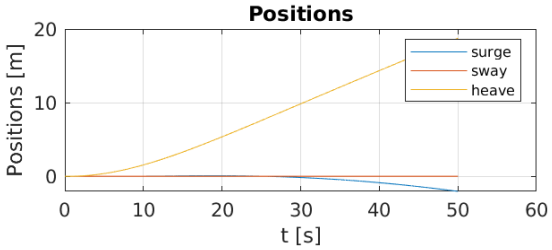

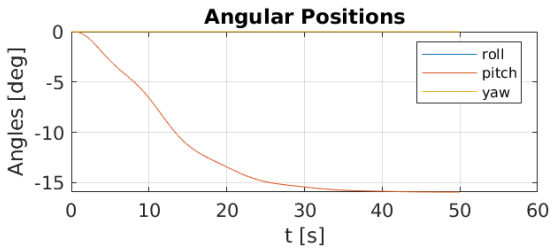

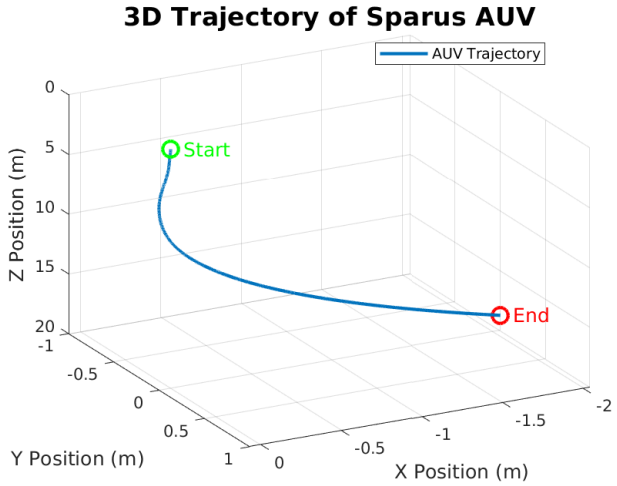

It can be noticed that, with the same strength of the thruster at 20%, a greater distance is achieved in the heave direction, increasing from 11 to 20 meters. This is due to the fact that the hull's drag forces are the most significant, as the hull covers the largest area. In addition, the pitch angle is higher since the thruster's force is acting solely to oppose the downward motion, creating a larger angle.

10.3.2 Impact of the antenna's drag forces

If the antenna's drag force is completely removed, its effect would be the most visible in the surge motion. This is because the antenna's largest projected area is the one x direction.

The following graphs show that the surge position reaches a higher value under the same thruster activation conditions (30% for the side thrusters and 0% for the middle thruster). The linear velocity also increases, as drag forces are proportional to the square of the velocity. However, both the angular position and angular velocity exhibit lower values. The reason was that the drag forces of the antenna were the main reason behind creating a pitch angle in the first place.

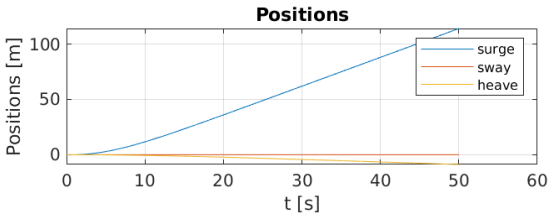

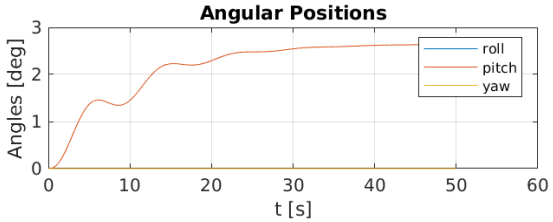

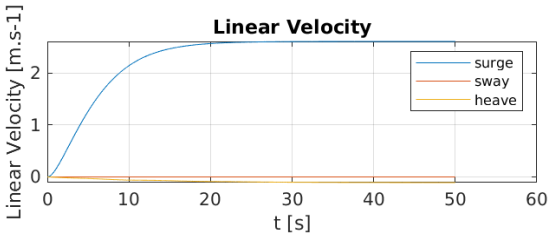

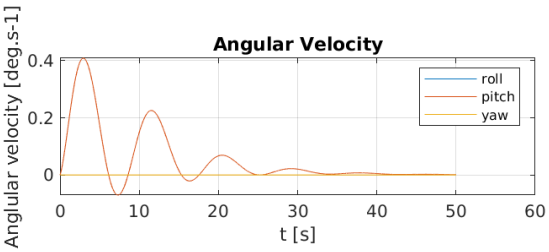

10.3.3 Impact of the thrusters' drag forces

The impact of the thrusters' drag forces is most noticeable in the heave motion. Replicating the scenario of a heave motion with 20% power from the middle thruster, without the thrusters' drag forces, the results differ significantly.

In the following graphs, it can be observed that the AUV oscillates in pitch between -1° and 1°, whereas, with the thruster's drag forces included, the pitch value decreases gradually to reach -4.5°. Similarly, the angular velocity for pitch oscillates between -1°/s and 1°/s, while under normal conditions, it is quickly damped to 0.

The thrusters' drag forces cause a higher pitch, but also by increasing damping, they make the system's response more predictable and easier for the PID controller to handle.

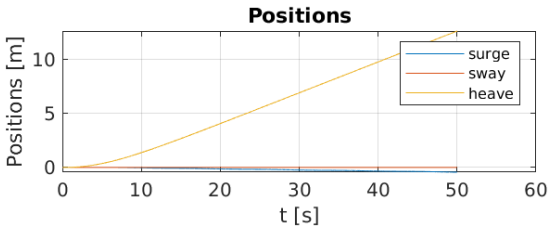

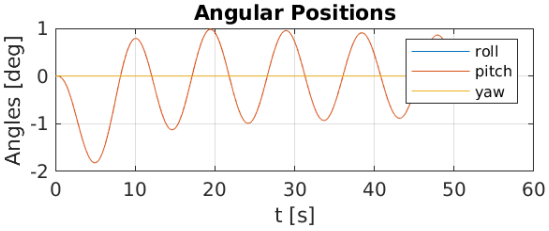

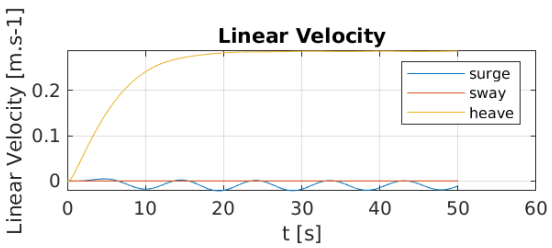

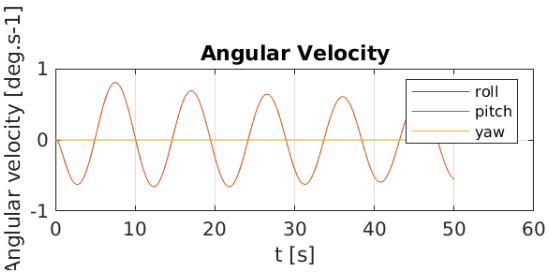

11 Conclusion

In conclusion, the modeling of an AUV requires several information about its body to provide the basis for calculating the general mass matrix (including the added mass matrices), as well as the drag matrices. Additionally, other forces, such as Coriolis forces, buoyancy (Archimedes' principle), and thrust, also significantly impact the AUV's dynamics.

The simulations produced demonstrate that the calculated parameters align with theoretical expectations of the AUV's behavior. Furthermore, they highlight the critical role of the mass matrices and drag forces in influencing the motion of a submerged vehicle.

This underscores the importance of accurately modeling an underwater vehicle to estimate its dynamic parameters. The use of mathematical tools, combined with a solid understanding of the vehicle's behavior under various conditions, is essential to develop a model that closely reflects reality.